

From Integrable to Chaotic Systems: Universal Local Statistics of Lyapunov exponents

Gernot Akemann*

Faculty of Physics, Bielefeld University, Postfach 100131, D-33501 Bielefeld, Germany

Zdzislaw Burda†

*Faculty of Physics and Applied Computer Science,
AGH University of Science and Technology, al. Mickiewicza 30, PL-30059 Krakow, Poland*

Mario Kieburg‡

Faculty of Physics, University of Bielefeld, Postfach 100131, D-33501 Bielefeld, Germany

(Dated: July 8, 2022)

Multi-layered complex systems appear nowadays in many applications, ranging from quantum systems to machine learning. A major question is about their stability, which is partially encoded in the Lyapunov exponents. We study their microscopic spectral statistics, resulting from the product of M complex Ginibre random matrices of sizes $N \times N$. In a double scaling limit for $N, M \rightarrow \infty$ they exhibit a rich variety of correlations and we argue that this behaviour is universal, and thus to be seen in applications. Depending on the relation between N and M , we find a deterministic ($M \gg N$) and a probabilistic regime ($M \ll N$). On the scale of the local mean level spacing the former shows picket fence statistics, the sum of equally spaced eigenvalues known from the quantum harmonic oscillator, which is integrable. In contrast, the probabilistic regime follows the universal statistics of the classical Gaussian Unitary Ensemble (GUE) of random matrices, describing quantum chaotic systems. At the transition, when imposing a critical scaling $M \propto N$, we find two new classes of statistics. They interpolate between the deterministic and the GUE sine- or Airy-kernel, depending on the location in the spectrum. Our analytical computations are based on the representation of the product matrix as a determinantal point process. The universality conjecture is corroborated by comparing with simulations for other kinds of random matrix products.

Introduction. Products of random matrices are often applied to understand statistical properties of multi-layered complexity, describing the propagation of randomness through interactions between neighbouring layers. The class of multi-layered complexity embraces problems in the theory of dynamical systems in connection with the issue of stability, ergodicity and Lyapunov spectra [1, 2]; in thermal field theory and quantum propagation, where the underlying systems are described by products of transfer matrices or propagation kernels [3, 4]; in quantum entanglement [5]; in wireless telecommunication and information theory modelling information propagation through a sequence of MIMO channels [6, 7]; in machine learning in the analysis of the dynamical behaviour of deep neural network [8]; in disordered systems [9]; in studies of complexity of random maps [10]; in machine inference based on hidden Markov chains [11]; in non-perturbative quantum gravity with space-time foliation [12]; in multiplex networks [13] and in many other fields. The way how the products are implemented depends on the specific problem and requires a case-by-case study. However, many properties of random matrices and their products are highly universal in the limit of large matrix size. We want to shed some light on detailed generic properties of the multi-layered complexity when both, dimension and number of matrices multiplied, become large.

Products of random matrices have been studied since the sixties [14, 15]. These studies have mainly concen-

trated on limiting laws for products of $N \times N$ dimensional matrices in the limit of a large number $M \rightarrow \infty$ of matrices multiplied. It is convenient to think of N as the number of degrees of freedom per layer, and of M as the number of layers or, alternatively, as the numbers of spatial and temporal degrees of freedom, respectively. A special case is the product of complex Ginibre matrices [16], square complex matrices with independent identically distributed (i.i.d.) normal random variables [17, 18] as entries. In this case one can determine the spectrum of Lyapunov exponents in the limit $M \rightarrow \infty$, cf. [19] for a recent summary of mathematical results. Recently, exact analytical expressions for the joint probability distribution functions of the eigenvalues [20] and singular values [7, 21] have been derived for finite M and N . The underlying structure of a determinantal point process [22] has proven to be very fruitful, as all k -point correlation functions are given by

$$R_k(x_1, \dots, x_k) = \det[K(x_j, x_l)]_{j,l=1,\dots,k}, \quad (1)$$

with correlation kernel $K(x_j, x_l)$ and level density $R_1(x) = K(x, x)$. For Ginibre matrices [7, 21] it is expressed in terms of Meijer G-functions [23]. These findings have initiated considerable activity, leading to an exact determination of all correlations for finite M and $N \rightarrow \infty$, see e.g. [24, 25] and references in the review [26]. An alternative measure in random matrix theory is the nearest neighbour spacing distribution, see [27] for a recent application to Lyapunov spectra.

Here, we derive the full local spectral statistics for the Lyapunov exponents in a double scaling limit (dsl) $M, N \rightarrow \infty$. Such limits can be understood as continuum limits in space and time. In [28], we have argued that when taking first $M \rightarrow \infty$ and then $N \rightarrow \infty$ the local spectral statistics is that of a quantum harmonic oscillator, named picket fence statistics in [29]. In contrast, taking first $N \rightarrow \infty$ and then $M \rightarrow \infty$, should yield the universal local statistics of the Gaussian Unitary Ensemble (GUE) associated to quantum systems that are K -chaotic in the classic world [29]. Relating picket fence statistics with the onset of an integrable quantum system and, hence, complementing the Berry-Tabor conjecture [30], products of operators can undergo a transition. We determine the spectral statistics at such a transition for systems represented by operators without further symmetries, by choosing complex Ginibre matrices.

Qualitative Discussion. We consider $M + 1$ layers of the system, where each layer is described by an N -dimensional vector v_j , $j = 0, \dots, M$. In the simplest situation $v_j = X_j v_{j-1}$, the evolution from an initial condition v_0 to the M 'th layer follows the product $X_M \cdots X_1$. Much information is encoded in the Lyapunov exponents being eigenvalues of the *Lyapunov matrix*

$$L = \frac{1}{2M} \log(X_M \cdots X_1)^\dagger (X_M \cdots X_1). \quad (2)$$

Invertibility of the product is assumed throughout this work.

Let us consider an arbitrary product of operators, without prior assumption about their dependence. While our explicit calculations are for Ginibre matrices, our discussion should apply to more general situations. As an example, in Fig. 3, we compare the microscopic level density in the bulk of the spectrum of the product of Ginibre matrices, complex Bernoulli matrices (with entries $0, \pm 1, \pm i, \pm 1 \pm i$), and sums of Ginibre matrices A_j , $X_j = A_j + A_{j-1}$ with $A_0 = 0$. The latter choice can be understood as a model for progressive scattering with a short memory, making it non-Markovian. For $M = 2$ it was considered in [31].

In several works, e.g. [17, 32–35], it has been shown for various kinds of X_j being i.i.d. that the distributions of the Lyapunov exponents λ_j become asymptotically Gaussian when $M \gg N$. The level density is

$$R_1(\lambda) \approx \sum_{j=1}^N \frac{1}{\sqrt{2\pi\sigma_j^2}} \exp\left[-\frac{(\lambda - \bar{\lambda}_j)^2}{2\sigma_j^2}\right], \quad (3)$$

with deterministic means $\bar{\lambda}_j$ [17] and standard deviations σ_j . For Ginibre they are given by [28]

$$\bar{\lambda}_j = \frac{\psi(j)}{2} \quad \text{and} \quad \sigma_j = \sqrt{\frac{\psi'(j)}{4M}}, \quad (4)$$

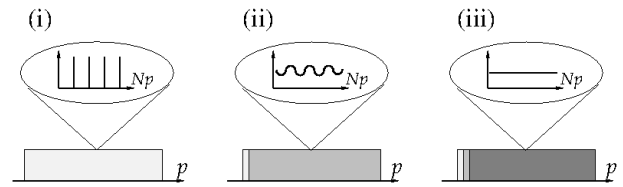


Figure 1. Sketches of the unfolded microscopic spectra (insets) of the Lyapunov exponents in different dsl: (i) $M \gg N$, (ii) $M \propto N$, and (iii) $M \ll N$. The ratio $p = j/N \in [0, 1]$, labels the number j of ordered eigenvalues. Picket fence statistics is in light grey, the interpolating dsl in grey, and GUE statistics in dark grey.

where $\psi(z) = (\log \Gamma(z))'$ is the digamma function [23]. When $N/M \rightarrow 0$ the level density becomes a sum of Dirac delta functions, corresponding to picket fence statistics after proper unfolding.

Clearly, the approximation (3) holds as long as the overlap between individual Lyapunov exponents is small, meaning the j th *width-to-spacing-ratio* (WSR) defined by

$$\text{WSR}_j = \frac{1}{2} \frac{\sigma_j + \sigma_{j-1}}{\bar{\lambda}_j - \bar{\lambda}_{j-1}}, \quad \text{for Ginibre } \text{WSR}_j \stackrel{j \gg 1}{\approx} \sqrt{\frac{j}{M}}, \quad (5)$$

is small. In the case of M Ginibre matrices this is always satisfied when j is fixed while $N, M \rightarrow \infty$ (hard edge scaling, lower bound), regardless of any relation between N and M . In contrast, for the largest, N th Lyapunov exponent, $\text{WSR}_N \approx \sqrt{N/M}$ is only small when $M \gg N$. For $M \ll N$ we cannot expect the approximation (3) to hold; the overlap between individual eigenvalue distributions becomes large, their interaction dominant and the standard GUE results [36] should follow. The critical regime is when $M \propto N$ or more precisely $M \propto j$.

Hence, we obtain the following picture illustrated in Fig. 1 for the product of M Ginibre matrices as discussed in detail in the ensuing paragraphs. When studying the dsl $M, N \rightarrow \infty$ with the relation $a = \lim_{N \rightarrow \infty} N/M$, we find three distinct asymptotic regimes: (i) $M(N)$ increasing super-linearly ($a = 0$), (ii) linearly ($0 < a < \infty$), or (iii) sub-linearly ($a = \infty$) with N . This identification of scales is our first main result. Below we will only consider the bulk and soft edge (upper bound) of the Lyapunov exponents as they display new features. The local WSR is parametrised by a as $\text{WSR}_{j=Np} = \sqrt{ap}$, see (5). It increases when moving from left to right in the spectrum, cf. Fig. 1. A similar picture is expected for a general product of operators, with the WSR as a parameter, cf. Fig. 3.

Unfolding for Ginibre. To compare microscopic properties of different spectra one needs to unfold them [37]. The averaged cumulative density

$$\bar{N}(\lambda) = \int_{-\infty}^{\lambda} \bar{R}_1(\lambda') d\lambda', \quad (6)$$

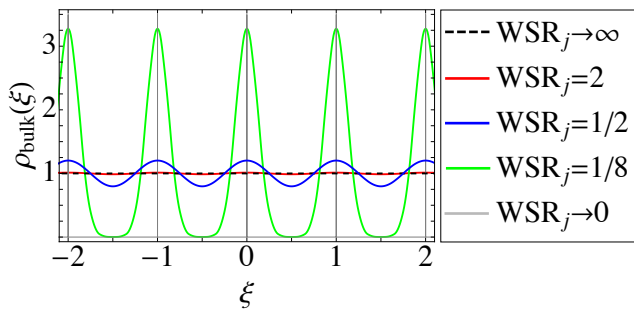


Figure 2. The unfolded microscopic level density (11) in the bulk for various values of $\text{WSR}_j = \sqrt{j/N} = \sqrt{ap}$, where we have set $\Delta p = 0$ as discussed in the text. The origin represents the point where we zoom in. The limiting constant density (dashed) corresponds to the sine-kernel.

has to be determined, with $\bar{R}_1(\lambda)$ being the non-fluctuating part of the level density, approaching the macroscopic level density at $N \rightarrow \infty$. When no analytical formulas for $\bar{R}_1(\lambda)$ and $\bar{N}(\lambda)$ are available, e.g. for comparison with experimental data, one has to perform a fit, see e.g. [37]. Fortunately, for products of Ginibre matrices analytical formulas for $R_1(\lambda)$ exist [7]. The eigenvalue statistics of the random matrix $\exp[2ML]$ follows a determinantal point process at fixed M and N , cf. (1), with kernel

$$K(x, y) = \frac{1}{x} \sum_{j=1}^N \left(\frac{x}{y}\right)^j G_j(y), \quad (7)$$

$$G_j(y) = \int_{-i\infty}^{+i\infty} \frac{dt}{2\pi i} \frac{\sin(\pi t)}{\pi t} y^t \left(\frac{\Gamma(j-t)}{\Gamma(j)}\right)^{M+1} \times \frac{\Gamma(N-j+1+t)}{\Gamma(N-j+1)}. \quad (8)$$

Here, G_j is essentially a Meijer G-function following from an equivalent representation of the kernel in [21]. The normalized level density of L is then

$$\frac{1}{N} R_1(\lambda) = \frac{2M}{N} e^{2M\lambda} K(e^{2M\lambda}, e^{2M\lambda}) = \frac{2M}{N} \sum_{j=1}^N G_j(e^{2M\lambda}). \quad (9)$$

The prefactor stems from the Jacobian of the unfolding. Similarly, the k -point correlation functions (1) of L are given by the kernel $2Me^{2M\lambda_j} K(e^{2M\lambda_j}, e^{2M\lambda_i})$.

Due to the explicit form of the kernel (7) we can take various limits. For fixed N and sufficiently large M one reproduces the Gaussian result (3): For $y = e^{2M\lambda}$, the integral (8) picks up its main contribution from the saddle point at $t = 0$. When $M \rightarrow \infty$ with finite j , this yields a Dirac delta at $\bar{\lambda}_j = \psi(j)/2$. Thence, the spectrum at the hard edge is always discrete and deterministic on a microscopic scale and, after proper unfolding, gives picket fence statistics.

The unfolding follows from the asymptotic behaviour of the eigenvalues of the matrix e^{2L}/N which are approximately $e^{\psi(j)}/N$. For $j = Np$ with $p \in (0, 1)$ being of order N , the limiting form is $e^{\psi(j)}/N \approx p$ for $N \rightarrow \infty$, following from the asymptotic formula $\psi(Np) \approx \log(N) + \log(p) + \mathcal{O}(1/N)$. Thus, the eigenvalues $p = e^{2\lambda}/N$ are uniformly distributed on $(0, 1)$. This only holds when being away from the edges at $p = 0, 1$. The map $\lambda \mapsto p$ is just the cumulative distribution (6) (quantile) and therefore the proper unfolding.

Bulk Statistics. Zooming into the microscopic scale in the bulk at $p \in (0, 1)$ we consider two neighbouring points $x = (Np + \xi)^M$ and $y = (Np + \zeta)^M$ in the kernel (7), with ξ and ζ of order unity. Multiplied with the Jacobian $M(Np + \xi)^{M-1}$ the kernel (7) in the bulk becomes

$$\begin{aligned} & K_{\text{bulk}}(\xi, \zeta; a) \\ &= \lim_{N, M \rightarrow \infty} M(Np + \xi)^{M-1} \frac{g(\xi)}{g(\zeta)} K(x, y) \\ &= \frac{1}{2\pi ap} \sum_{j=-\infty}^{+\infty} \exp\left[\frac{j(\xi - \zeta)}{ap}\right] \\ &\quad \times \text{Re}\left(\text{erfi}\left[\frac{\pi\sqrt{2ap}}{2} + i\frac{1}{\sqrt{2ap}}(\zeta - \Delta p - j)\right]\right), \end{aligned} \quad (10)$$

for $a = \lim_{N, M \rightarrow \infty} N/M \in (0, \infty)$. This is our second main result. Here, $g(\xi)$ is an appropriate function to guarantee the existence of the limit. It drops out for any k -point correlation function (1). The imaginary error function is denoted by $\text{erfi}(z) = \frac{2}{\sqrt{\pi}} \int_0^z \exp[t^2] dt$. The local shift $\Delta p = Np - [Np] + 1/2 - ap \log[(1-p)/p] - ap$ is model dependent and thus not universal. It encodes how far we are away from the origin and what the distance of Np to the closest integer $[Np]$ is.

The microscopic level density on the scale of the local mean level spacing is then determined by the relation

$$\rho_{\text{bulk}}(\xi; a) = K_{\text{bulk}}(\xi, \xi; a). \quad (11)$$

The behaviour of $\rho_{\text{bulk}}(\xi; a)$ is shown in Fig. 2. A comparison to Monte Carlo simulations of three different products of random matrices is given in Fig. 3. The interpolating microscopic density in the bulk (11) as well as the corresponding kernel (10) enjoy a discrete periodicity on a local scale, i.e. $\rho_{\text{bulk}}(\xi; a) = \rho_{\text{bulk}}(\xi + 1; a)$. A full continuous translation invariance [25] is restored only in the limit $a \rightarrow \infty$ where one recovers the sine-kernel [36]

$$K_{\text{sin}}(\xi, \zeta) = \frac{\sin[\pi(\xi - \zeta)]}{\pi(\xi - \zeta)} = \lim_{a \rightarrow \infty} K_{\text{bulk}}(\xi, \zeta; a). \quad (12)$$

The limit follows from approximating the sum (10) by an integral that can be performed. Yet, there is still a small region between the hard edge and the bulk even for $a \rightarrow 0$ where the transition kernel (11) can be still found. We recall that WSR_j , see (5), or equivalently $ap = j/M = \text{WSR}_j^2$ enters in the kernel (11).

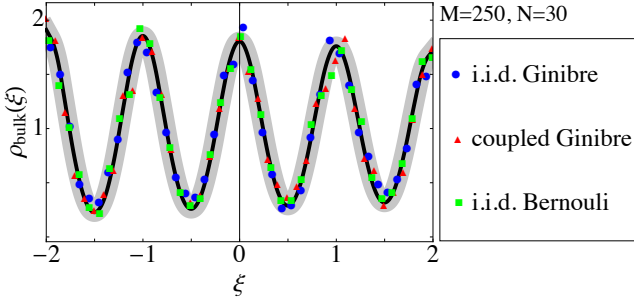


Figure 3. Comparison of Monte Carlo simulations (symbols) of three matrix products introduced after (2), at $M = 250$, $N = 30$, with the analytical result (11) at $\text{WSR}_{j=15} \approx 0.24$ (black curve). Each product ensembles comprises 1192 configurations, with a residual statistical error of about 10% (grey area). Because of the small matrix dimension $N = 30$, we expect further deviations for the chosen eigenvalues $j = 13, \dots, 17$. To improve the fit we replaced $p = 15/30 = 0.5$ by $p = (15 + \xi)/30$ in (11).

For $a \rightarrow 0$ the expression (11) reduces to a sum of Dirac delta functions,

$$\lim_{a \rightarrow 0} \rho_{\text{bulk}}(\xi; a) = \sum_{j=-\infty}^{\infty} \delta(\xi - \Delta p - j), \quad (13)$$

because the erfi-function approximately narrows to a Gaussian. The same applies to any k -point correlation function, yielding picket fence statistics [29].

Soft Edge Statistics. At the edges the mean level spacing has a different scaling behaviour. For the soft edge $p = 1$, we adopt the finite M scaling of [25] and find the position of the upper spectral edge of $\exp[2ML]$ at $N^M(M+1)^{M+1}/M^M$, when $N \rightarrow \infty$. The probability of finding an eigenvalue above the edge drops exponentially. Therefore, we zoom into the spectrum as

$$x = \frac{(M+1)^{M+1}}{M^M} N^M \left(1 + \left(\frac{M}{N} \right)^{2/3} \frac{\xi}{M} \right)^M. \quad (14)$$

The prefactor $(M/N)^{2/3}$ in front of ξ is reminiscent to the Airy-kernel scaling [36]. We insert this scaling into (7) and fix the limit $a = \lim_{N, M \rightarrow \infty} N/M$. Then, the dsl $M, N \rightarrow \infty$ (14) leads to the interpolating kernel,

$$\begin{aligned} & K_{\text{soft}}(\xi, \zeta; a) \\ &= \lim_{N, M \rightarrow \infty} \frac{1}{a^{2/3}} \left(1 + \frac{\xi}{Ma^{2/3}} \right)^{M-1} \frac{\tilde{g}(\xi)}{\tilde{g}(\zeta)} K(x, y) \\ &= \int_{\mathcal{C}} \frac{dt}{2\pi i a^{2/3}} \frac{(1 - \exp[-t/a - (\xi - \zeta)/a^{1/3}])^{t-1}}{\Gamma(1+t)} \\ & \quad \times \exp \left[t^2 - t \left(1 - \log a + \frac{1}{2a} + \frac{\zeta}{a^{2/3}} \right) \right], \end{aligned} \quad (15)$$

our third main result. The contour \mathcal{C} is given by the shifted imaginary axis $i\mathbb{R} + 1/2$. The interpolating microscopic level density at the soft-edge reads $\rho_{\text{soft}}(\xi; a) =$

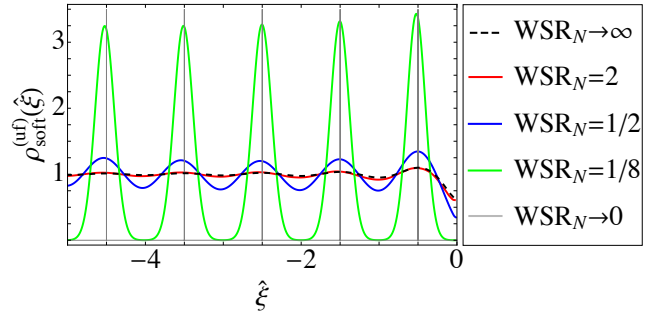


Figure 4. The interpolating microscopic level density at the soft edge from (15) after unfolding (uf), for various values of $\text{WSR}_N = \sqrt{a}$, with the upper bound of the macroscopic density at zero. After unfolding the limiting Airy-density (17) is only weakly oscillating (dashed).

$K_{\text{soft}}(\xi, \zeta; a)$. We expect that these statistics will also hold for more general products of operators, as long as a soft edge is present.

For $a \rightarrow \infty$, we recover the GUE Airy-kernel [36],

$$\begin{aligned} K_{\text{Airy}}(\xi, \zeta) &= \lim_{a \rightarrow \infty} \frac{\hat{g}(\xi)}{\hat{g}(\zeta)} K_{\text{soft}}(\xi, \zeta; a) \\ &= 2^{-1/3} \frac{\text{Ai}(2^{1/3}\xi)\text{Ai}'(2^{1/3}\zeta) - \text{Ai}(2^{1/3}\zeta)\text{Ai}'(2^{1/3}\xi)}{\xi - \zeta} \end{aligned} \quad (16)$$

depending on the Airy function. For the interpolating level density at the soft edge we have the limit

$$\lim_{a \rightarrow \infty} \rho_{\text{soft}}(\xi; a) = 2^{1/3} \text{Ai}'^2(2^{1/3}\xi) - 2^{2/3} \xi \text{Ai}^2(2^{1/3}\xi). \quad (17)$$

We would like to emphasize that just like the Airy-kernel (16) the spectrum of (15) is still not yet properly unfolded. For example, for large argument ξ , the limiting Airy-density (17) increases as $\sqrt{|\xi|}$ to the left, originating from the macroscopic semi-circular density of the GUE.

In Fig. 4 we compare the unfolded density for the interpolating kernel (15) and the Airy-density. Note that our unfolding is only valid inside the support of the macroscopic level density. For the tails, which include the Tracy-Widom distribution [38], a different means of comparison has to be sought.

In the opposite limit, for $a \rightarrow 0$, we rescale $\xi = \hat{\xi}/a^{1/3}$,

$$\lim_{a \rightarrow 0} \frac{1}{a^{1/3}} \rho_{\text{soft}} \left(\frac{\hat{\xi}}{a^{1/3}}; a \right) = \sum_{j=1}^{\infty} \delta \left(\hat{\xi} + j - \frac{1}{2} \right). \quad (18)$$

This is the picket fence statistics and hence the spectrum of a quantum harmonic oscillator. The rescaling by $a^{-1/3}$ is essential to get a normalized mean level spacing. It is well known that the largest eigenvalue distribution of the Airy-density (17) is given by the Tracy-Widom distribution [38]. In contrast, in the picket fence limit the largest

eigenvalue is approximately Gaussian, see (3). The interpolating kernel (15) thus describes an interpolation between the two, demanding further investigations.

Conclusions. We have discussed local statistical properties of Lyapunov exponents resulting from products of M random matrices of size N in various limits. Our first result was to identify the double scaling limit $N, M \rightarrow \infty$, where M typically represents the number of layers or times steps and N the degrees of freedom and thus the complexity of the underlying system. We found that a linear relation $a \propto N/M$ separates two different regimes, associated with integrable or chaotic behaviour. When $M \gg N$ the entire Lyapunov spectrum becomes deterministic and can be mapped to a picket fence, thus corresponding to the integrable harmonic oscillator. In the opposite limit $M \ll N$, for the bulk and the largest Lyapunov exponents at the soft edge of the spectrum we found classical random matrix statistics of the GUE, associated with quantum chaotic behaviour. In the critical regime two families of a -dependent correlations interpolate between the sine- and Airy-kernel of the GUE and the picket fence, respectively. We have identified our scaling parameter a as the squared width-to spacing-ratio of Lyapunov exponents, aiming at general applications. The claimed universality of our analytical findings was substantiated by comparison with numerical simulations of different random matrix products.

Apart from applications to realistic dynamical systems, where such a transition should be identified, several more theoretical questions remain open. A standard quantity in measuring chaotic behaviour is the nearest neighbour spacing distribution. In the integrable limit the equal spacing of the unfolded level density is described by a Dirac delta rather than a Poisson distribution. The shape of such a transition, starting from the Wigner surmise, is worth investigating. Second, the supposedly exponential tail of the distribution of the largest Lyapunov exponent has important consequences for the stability of the system and its Kaplan-Yorke dimension [39]. Our interpolating Airy-kernel suggests a transition from the Tracy-Widom distribution to a Gaussian that could be observable.

Acknowledgements. We acknowledge support by the German research council (DFG) through CRC 1283: "Taming uncertainty and profiting from randomness and low regularity in analysis, stochastics and their applications" (GA,MK) and by the AGH UST statutory tasks No. 11.11.220.01/2 within subsidy of the Ministry of Science and Higher Education (ZB). We thank D.-Z. Liu and D. Wang for sharing their results about the same double scaling limit at the soft edge, especially we are grateful for D.-Z. Liu's comments on a preprint version of this letter.

-
- * akemann@physik.uni-bielefeld.de
† zdzislaw.burda@agh.edu.pl
‡ mkieburg@physik.uni-bielefeld.de
- [1] V. I. Oseledec, *Trans. Moscow Math. Soc.* **19**, 197 (1968).
 - [2] L. Arnold, *Random Dynamical Systems*, Springer, Berlin (1998).
 - [3] R. A. Janik and W. Wieczorek, *J. Phys. A* **37**, 6521 (2004) [arXiv:math-ph/0312043].
 - [4] P. Bougerol and J. Lacroix, *Products of Random Matrices with Applications to Schrödinger Operators*, Birkhäuser, Basel (1985).
 - [5] B. Collins, I. Nechita and K. Zyczkowski, *J. Phys. A* **43**, 275303 (2010) [arXiv:1003.3075].
 - [6] R. R. Mueller, *IEEE Trans. Inf. Theor.* **48**, 2086 (2002).
 - [7] G. Akemann, M. Kieburg, and L. Wei, *J. Phys. A* **46**, 275205 (2013) [arXiv:1303.5694].
 - [8] H. Li, *Analysis on the Nonlinear Dynamics of Deep Neural Networks: Topological Entropy and Chaos*, arXiv:1804.03987 (2018).
 - [9] A. Crisanti, G. Paladin, and G. A. Vulpiani, *Products of Random Matrices in Statistical Physics*, Springer, Berlin (1992).
 - [10] J. R. Ipsen and P. J. Forrester, *Kac-Rice fixed point analysis for single- and multi-layered complex systems*, arXiv:1807.05790 (2018).
 - [11] O. Cappé, E. Moulines, and T. Rydén, *Inference in hidden Markov models*, Vol. **6**, Springer, Berlin (2005).
 - [12] J. Ambjørn, J. Jurkiewicz, and R. Loll, *Phys. Rev. Lett.* **95**, 171301 (2005) [arXiv:hep-th/0505113].
 - [13] S. Gómez, A. Díaz-Guilera, J. Gómez-Gardeñes, C. J. Pérez-Vicente, Y. Moreno, and A. Arenas, *Phys. Rev. Lett.* **110**, 028701 (2013) [arXiv:1207.2788].
 - [14] H. Furstenberg and H. Kesten, *Ann. Math. Statist.* **31**, 457 (1960).
 - [15] J. E. Cohen, H. Kesten, and C.M. Newman (eds.), *Random matrices and their applications*, Contemporary Mathematics Vol. **50**, American Mathematical Society, Providence, RI, (1986).
 - [16] J. Ginibre, *J. Math. Phys.* **6**, 440 (1965).
 - [17] C. M. Newman, *Commun. Math. Phys.* **103**, 121 (1986).
 - [18] M. Isopi and C. M. Newman, *Commun. Math. Phys.* **143**, 591 (1992).
 - [19] M. Viana, *Lectures on Lyapunov Exponents*, Cambridge Uni. Press, Cambridge (2014).
 - [20] G. Akemann and Z. Burda, *J. Phys. A* **45**, 465201 (2012) [arXiv:1208.0187].
 - [21] G. Akemann, J. R. Ipsen, and M. Kieburg, *Phys. Rev. E* **88**, 052118 (2013) [arXiv:1307.7560].
 - [22] K. Johansson, *Random matrices and determinantal processes*, in *Mathematical Statistical Physics* **83**, A. Bovier et al. (eds), Les Houches Summer School 2005, Session LXXXIII, Elsevier, Amsterdam (2006) [arXiv:math-ph/0510038].
 - [23] F. W. J. Olver, A. B. Olde Daalhuis, D. W. Lozier, B. I. Schneider, R. F. Boisvert, C. W. Clark, B. R. Miller, and B. V. Saunders, *NIST Digital Library of Mathematical Functions*, Release 1.0.15 of 2017-06-01, <http://dlmf.nist.gov/>.
 - [24] A. B. J. Kuijlaars and D. Stivigny, *Random Matrices: Theory and Applications* **3**, 1450011 (2014) [arXiv:1404.5802].

- [25] D.-Z. Liu, D. Wang, and L. Zhang, *Ann. de L'Institut Henri Poincaré - Probabilités et Statistiques* **52**, 1734 (2016) [arXiv:1412.6777].
- [26] G. Akemann and J. R. Ipsen, *Acta Phys. Pol. B* **46**, 1747 (2015) [arXiv:1502.01667].
- [27] M. Hanada, H. Shimada, and M. Tezuka, *Phys. Rev. E* **97**, 022224 (2018) [arXiv:1702.06935].
- [28] G. Akemann, Z. Burda, and M. Kieburg, *J. Phys. A* **47**, 395202 (2014) [arXiv:1406.0803].
- [29] O. Bohigas, M.J. Giannoni, and C. Schmit, *Phys. Rev. Lett.* **52**, 1 (1984); *Journal de Physique Lettres* **45**, 1015 (1984).
- [30] M. V. Berry and M. Tabor, *Proc. Roy. Soc. A* **356**, 375 (1977).
- [31] G. Akemann and E. Strahov, *Ann. Henri Poincaré* **19**, 2599 (2018) [arXiv:1711.01873].
- [32] V. V. Sazonov; V. N. Tutubalin, *Theor. Prob. Appl.* **11**, 1 (1966).
- [33] D. S. P. Richards, *J. Multivariate Anal.* **29**, 326 (1989).
- [34] N. K. Reddy, *International Mathematics Research Notices*, rnx134 (2017) [arXiv:1601.02888 [math.PR]].
- [35] M. Kieburg and H. Kösters, *Annales de l'Institut Henri Poincaré B* in press, arXiv:1601.03724 (2016).
- [36] M. L. Mehta, *Random Matrices*, 3rd ed., Elsevier, Amsterdam (2004).
- [37] T. Guhr, A. Müller-Groeling, and H. A. Weidenmüller, *Phys. Rept.* **299**, 189 (1998) [arXiv:hep-ph/9701387].
- [38] C. A. Tracy and H. Widom, *Commun. Math. Phys.* **159**, 151 (1994) [arXiv:hep-th/9211141].
- [39] J. Kaplan and J. Yorke, *Chaotic behavior of multidimensional difference equations*, in H. O. Peitgen, and H. O. Walther (eds.), *Functional Differential Equations and Approximation of Fixed Points*, Springer, Berlin (1979).